12TH INTERNATIONAL SYMPOSIUM ON FLOW VISUALIZATION
September 10-14, 2006, German Aerospace Center (DLR), Göttingen, Germany

# HYBRID APPROACH BETWEEN EXPERIMENT AND EVALUATION FOR ARTEFACT DETECTION AND FLOW FIELD RECONSTRUCTION – A NOVEL APPROACH EXEMPLIFIED ON MICROORGANISMIC INDUCED FLUID FLOWS

**H. Petermeier[1], A. Delgado[2] , P. Kondratieva[3], R. Westermann[3], F. Holtmann[4], V.V.Krishnamachari[4], C. Denz[4]**

**[1] Technische Universität München , InformationsTechnologie Weihenstephan, Am Forum 1, 85354 Freising**

**[2]Friedrich-Alexander-Universität Erlangen-Nürnberg, Lehrstuhl für Strömungsmechanik, Cauerstr. 4, 91058 Erlangen**

**[3] Technische Universität München, Computer Graphics & Visualization, Boltzmannstr. 3, 85748 Garching**

**[4]Westfälische Wilhelms-Universität Münster, Institut für Angewandte Physik, Correnstr. 2, 48149 Münster**

***Keywords*: optical novelty filtering, graphical processing unit, neural network, hybrid, artefact detection**

## ABSTRACT

*In biological fluid mechanics powerful image acquisition systems which guarantee biocompatibility are required for making progress towards a better understanding of natural phenomena being optimized by evolution in nature. For this advanced evaluation methods enabling the sophisticated analysis and description of flow fields are also necessary. In the present contribution, a novel so called neurohybrid is presented which allows detecting artefacts in experimental PIV data of microorganismic flow fields caused by ciliates. The management of artefacts is performed by the neurohybrid using a priori knowledge of the flow physics formulated in numerical expressions and the enormous potential of artificial neural networks in predicting artefacts and correcting them. In fact, a neuronumerical hybrid based on the physical knowledge provided by the Taylor-hypothesis can detect not only spurious velocity vectors but also additional phenomena like the contraction of the zooid.*

*This paper additionally deals also with a non-linear optical novelty filter which has decisive advantages in image processing as it automatically enhances the contrast of the biological tracer particles and removes quiescent image objects such as unavoidable dirt spots on the optical windows. Furthermore, the biocompatibility of novelty filtering has been shown to be excellent. Last but not least, model based reconstruction on GPU (Graphical Processing Unit) is proven to provide a powerful tool for recognizing data inconsistencies as well as for visualizing and analyzing flow field images.*

# 1 INTRODUCTION

Making substantial progress in biological fluid mechanics strongly depends on the availability of powerful optical whole field systems. Such systems as Particle Image Velocimetry (PIV) or Particle Tracking Velocimetry (PTV) for example, deliver images of the considered flow field. But unfortunately, artefacts introduced during the image processing substantially complicate the extraction of the velocity information. Thus, advanced evaluation methods for the analysis and description of flow fields are of vital interest. This is especially the case when flows induced by living microorganisms are studied as they impose considerable restrictions on the experimental setup and in the flow evaluation methods. To overcome these restrictions in the determination of the microorganismic flow field generated by ciliates the current work presents a biocompatible image generating method which manages artefacts by using a novel neuronumerical hybrid. For enhancing the quality of the captured images non-linear optical novelty filtering provides substantial advantages in comparison to the direct evaluation of the illuminated field usually done in PIV and PTV. Last but not least, the present contribution also proposes a model based approach for the reconstruction of flow fields from the image sequences implemented on the GPU (Graphical Processing Unit).

The underlying microorganismic induced flow field is generated by a peritrich ciliate, *opercularia asymmetrica*, which plays a vital role in biofilm growth. These ciliates generate a flow field to access the nutrients in the surrounding fluid by ciliary beating. The generated flow pattern shows a vortex ring inducing strong shear in the fluid. Apart this, the mass transport to the biofilm and thus also the nutrition of the biofilm is greatly influenced [1].

The restrictions on the experiment result from the necessity to keep biocompatibility. This means, any changes in the environment of the ciliates must be avoided, since the ciliates react very sensitive to them. Thus, the illumination may not be too powerful and the seeding density of the tracer particles is naturally limited, since the properties of the surrounding fluid will be influenced otherwise, to name only two influences. To handle and overcome these restrictions, a hybrid approach of both experimental and analysis methods is necessary. Fig. 1 gives an overview of this combination which will be explained in the following. Starting with the *experimental setup*, including the *cultivation* of the microorganisms as well as the *biotic tracer* particles in suitable *bioreactors,* the *sample* being analysed contains the *Opercularia Asymmetrica*. Basically, the phase contrast microscopy leads to *digital images* which are further processed using *PTV or PIV.* Subsequently, a *neurohybrid* approach is used for artefact detection. As an alternative, *optical novelty filter microscopy* [2] can be employed for generating images instead of phase contrast microscopy. An alternative flow field reconstruction based on

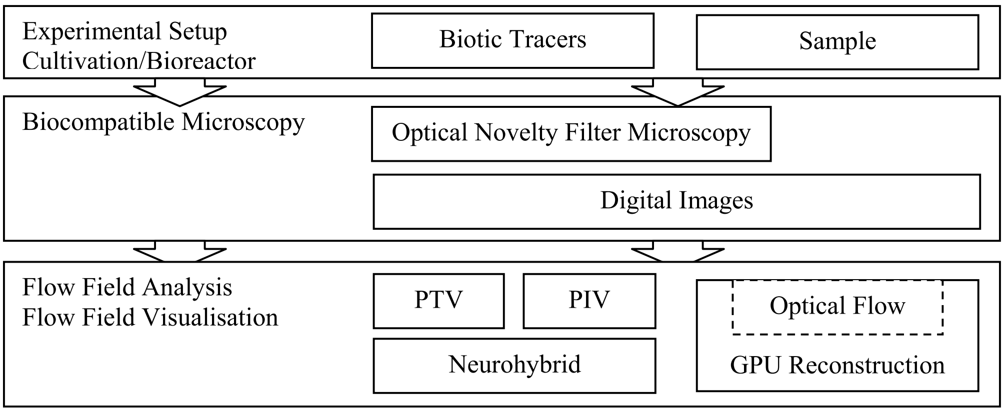


Fig. 1- Alternative images generating and evaluating investigated methods

*optical flow* method followed by the visualisation of the flow topology is performed in a step abbreviated with *GPU reconstruction* [3].

Apart from the particularities connected with biocompatibility and concerning the experimental setup, there are three main independent methods presented in this work.

*Neurohybrid* for artefact detection combines the learning ability of neural networks with basic fluid mechanical equations. Assuming that artefacts in image acquisition and image evaluation result in an additive error in the velocity field, the neural network learns a correcting velocity field necessary to minimize a Taylor-hypothesis based error term. As a result, the corrected velocity field is obtained. In combination with the local extrema of the Taylor-hypothesis error term it can also localize artefacts. Complementary to this approach, which computes the velocity field on an equidistant grid, velocity vectors from PTV are processed with another type of neurohybrid combining the information on an analytical solution which is valid in the vicinity of the ciliate. In this case, the neural network technique acts as a kind of model based parameter estimator for the analytical solution and detects the spurious vectors of the PTV evaluation.

*Optical novelty filtering (ONF)* using photorefractive crystals works as a temporal high pass filter blocking all information not changing with time instantaneously, i. e. background and thus reduces potential artefacts resulting from image acquisition. Furthermore, a novelty filter microscope provides images of amplitude as well as phase objects with increased contrast in comparison to conventional and phase contrast microscopes. Phase changes can be measured in real time with an accuracy of $\lambda/20$, with $\lambda$ as the wavelength of light used for microscopy. Additionally, the use of novelty filtering microscopy shows – concerning the biocompatibility – the great advantage of long term observations.

*GPU reconstruction* includes both the model-based reconstruction of the flow field and the interactive visualization of the flow topology. In addition to the implementation of the optical flow algorithm on the GPU to speed up the evaluation process, the development of a model-based approach for flow field reconstruction resulted in considerable advancements. A hybrid method including segmentation of flow cells in combination with an iterative correction step based on a direct Navier-Stokes solution indicates improved quality of the reconstructed fields. As this novel approach takes the fluid physics into account to constrain the velocity field, it is expected to automatically remove outliers and to resemble the real flow at much higher fidelity compared to previous approaches.

The alternative use of methods for emphasizing the adaptability of the developed neuronumerical hybrid provides a straightforward approach for the study of microbiological flows in detail as well as the analysis of flow fields in general.

## 2 ALTERNATIVE IMAGE MANAGEMENT APPROACHES AND DISCUSSION OF RESULTS

This section presents the methods outlined in the introduction and in Fig. 1 in detail. The datasets represent the motion of microorganisms of type ciliate in watery environment. Samples were taken from a sequencing batch bioreactor. The wastewater in this bioreactor is from a municipal wastewater treatment plant. For generating images via classical PIV or PTV a Zeiss Axiovert Microscope and a high speed CCD camera (MIKROTRON GmbH) with a maximum speed of 500 frames/sec with 12 microns pixel size are used. The flow induced by the motion of the microorganisms can be regarded as a Stokes flow. The characteristic Reynolds number is about

1.25·10$^{-3}$. For convenience, further details on the PIV or PTV evaluation, which represent the basis for the further recognition of artefacts represented in the following section, are given in [11]

## 2.1 Neurohybrid

The so called "functional nodes" applied in the present case were first used in bioprocess modelling [12]. The present case is a generalization of the previous approach using an analytical solution from literature as the functional nodes prior knowledge [13]. Fig. 2 shows the working principle of such a neurohybrid based on a feed-forward neural network with one functional node. The input layer feeds the independent variables to the network. Within a node the products of the output of the precedent nodes and the weigths of the connections are summed up, i. e. $n_i = \sum_{p \in P} a(n_p) w_{pi}$. Here $a(n_p)$ calculates the activation of the precedent node $n_p$. The activation functions are sigmoid shaped functions. The weighted connections in the hidden layers propagate the calculation forward through the net to the output layer.

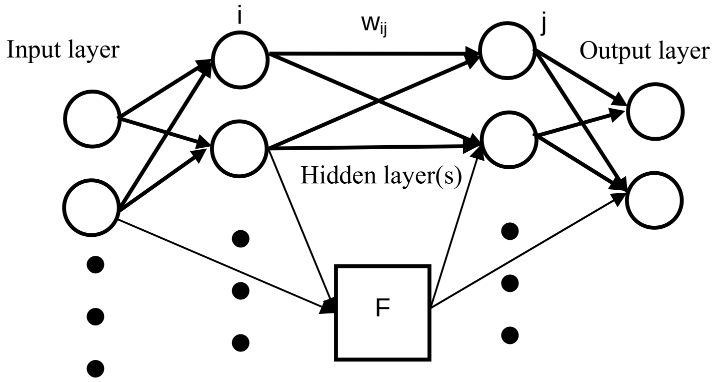


Fig. 2 – Sketch of a feed forward neural network. The circles represent classical nodes (neurons), the square a functional node. The weights are represented by $w_{ij}$ weighing the connection betweennode i and j.

During the training for each input vector the according output pattern $\vec{y}_i$ is confronted to the expected training pattern $\vec{t}_i$, in our case e. g. the velocity vectors obtained by a correlation based PIV algorithm. The error $\varepsilon = G(\|\vec{t}_i - \vec{y}_i\|)$ is calculated in a suitable norm, basically with the option to modify it with a quality function, which allows the introduction of additional penalty terms. The parameters of the map, i. e. the weights $w_{ij}$, are modified with the backpropagation algorithm, a gradient method, subseqently. The training is stopped when the training error falls below a prescribed bound (convergence).

Thus, artificial neural networks are a kind of approximators, and especially this property makes a lot of appliances feasible. But a trained network represents a black-box model. For this reason knowledge extraction – and integration – is hardly possible. In this case the use of functional nodes helps to overcome this restriction, since with this approach the nodes in the involved layers can be labelled with a physical meaning and thus a priori knowledge can be integrated into such networks.

The functional node F in Fig. 2 specifies the prior knowledge. The Taylor hypothesis [14] is chosen as additional fluid mechanical a priori knowledge, leading to a balance equation without taking external influences (forces) into account, especially in the case of laminar creeping flow. In particular, the spatial acceleration equals the temporal acceleration. Thus, for one velocity component, e. g. the x-component, the following equation holds

$$\left.\frac{\partial \tilde{u}}{\partial t}\right|_{(x_0,y_0)} + \left.\left( (u+\varepsilon_u)\frac{\partial \tilde{u}}{\partial x} + (v+\varepsilon_v)\frac{\partial \tilde{u}}{\partial y} \right)\right|_{(x_0,y_0)} = Ta(x_0,y_0)\,. \qquad (1)$$

Here the choice of one component is no restriction because of the coupling of the velocity components by the continuity equation. In equation 1 $(\varepsilon_u, \varepsilon_v)$ stands for the velocity field corrections. The temporal derivative $\tilde{u}_t$ as well as the spatial $\tilde{u}_x$ und $\tilde{u}_y$ and the velocity field $(\tilde{u}, \tilde{v})$ obtained e. g. from the PIV evaluation is used as training input. Of course, in a preprocessing step the temporal and spatial derivatives must be calculated using a propriate difference scheme from the velocity field $(\tilde{u}, \tilde{v})$. The output vector for each training pattern consists of a scalar $Ta(x_0, y_0)$ standing for the satisfaction of the Taylor-hypothesis which should be zero if the assumption holds and the corresponding velocity vector $(\tilde{u}, \tilde{v})$. So the correction velocity field $(\varepsilon_u, \varepsilon_v)$ depending on the position is kept in the artificial neural network part. The functional node gets $\tilde{u}, \tilde{v}, \tilde{u}_t, \tilde{u}_x, \tilde{u}_y, \varepsilon_u, \varepsilon_v$ as input. Consequently, the fulfilment of the Taylor-hypothesis is checked on the one hand, a comparison of the smoothened velocity field $(\tilde{u}+\varepsilon_u, \tilde{v}+\varepsilon_v)$ with the experimentally obtained velocity $(\tilde{u}, \tilde{v})$ field is computed using $\varepsilon^2 = (\varepsilon_u)^2 + (\varepsilon_v)^2 + (Ta)^2$ for error calculation on the other hand. Since the training error is dominated by the areas where the Taylor-hypothesis is not valid, not only image analysis artefacts but also time-varying boundary conditions can be detected as it is shown in Fig. 3. Thus, the neurohybrid shows a twofold benefit: the removal of spurious vectors with the help of the correction velocity field as well as the detection of other, "non-hydromechanical" phenomena like the contraction of a ciliate.

Although these findings prove the synergistic use of image processing by PIV/PTV and the Taylor-hybrid as an excellent method for determining the microorganismic flow field generated by ciliates, further methodological improvements are to be expected by implementing novelty filtering and model based visualization. This is illustrated in the following sections.

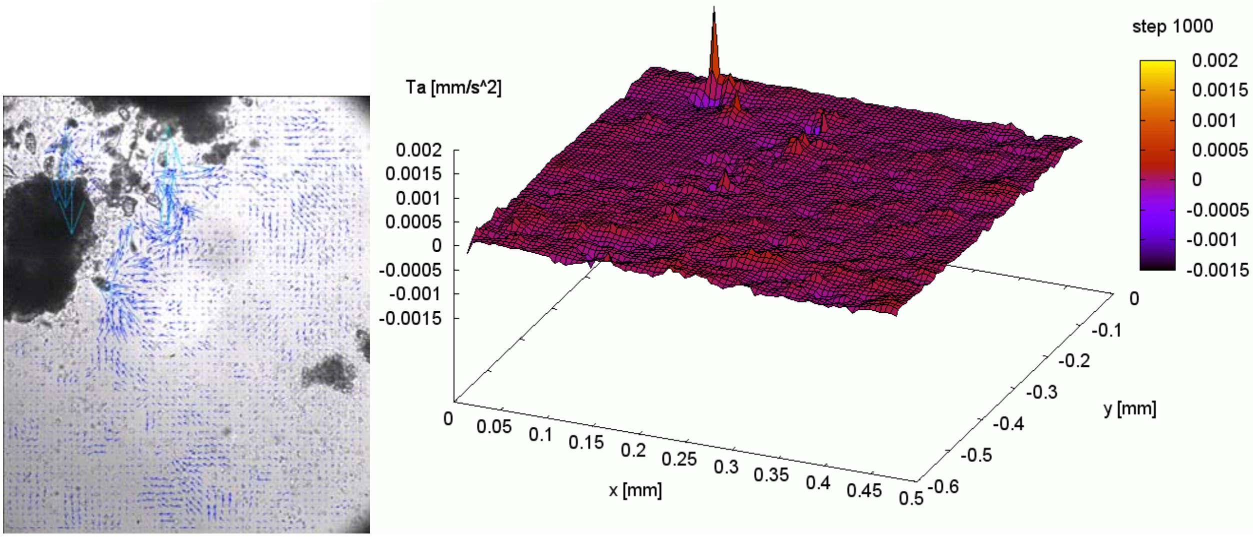


Fig. 3 – Flow situation as in Fig.s 3 and 4 with a larger scene. The dotted arrow highlights the contracting ciliate, the drawn through arrows the active ciliate.

## 2.2 Optical Novelty Filtering (ONF) as a nonlinear optical filtering technique

The photorefraction-based optical novelty filter [4] has been known for almost two decades. It is a temporal high pass filter [5] which detects only the dynamic portions in the field of view while suppressing the stationary background. Fig. 4 shows the sketch of the experimental implementation of a novelty filter microscope (NFM), which is later discussed in detail.

Photorefractive barium titanate ($BaTiO_3$) crystals are often employed to implement this filter. The most important highlight of this optical filter is that it is not only sensitive to amplitude changes but also to phase changes [6]. We demonstrated that the phase sensitivity of the device can be used to detect and measure the phase changes in real time introduced by moving phase objects with an accuracy of $\lambda/20$ [7,9]. In combination with a phase triggering technique [8], it is even possible to extend the phase measurement range to $2\pi$ radians. In microbiological fields objects are often transparent and thus phase objects. Hence the novelty filter can be used to get images of these objects with an increased signal to noise ratio in comparison to conventional or phase contrast microscopy. Because of the low intensities of only microwatts needed for novelty filtering, thus being biocompatible, the method can be used for long time observations of biological samples.

### *2.1.1 Photorefractive Novelty Filter Microscope (NFM)*

Fig. 4 shows the sketch of the experimental implementation of a NFM. A laser beam of wavelength 532nm derived from a frequency-doubled Nd:YAG laser, is split into a signal and a reference beam. The signal beam enters a conventional microscope and illuminates the object. The microscope objective and a projecting lens system produce a magnified image of the probe at the CCD camera. The images captured by the CCD camera are transferred to a PC for further analysis. The reference beam is made to interfere with the signal beam in a Ce-doped photorefractive $BaTiO_3$ crystal. The orientation of the c-axis of the crystal leads to a transfer of energy from the signal beam to the reference beam. This energy transfer results in a complete depletion of a static signal beam. Changes in the signal are not depleted thus being observed on the camera instantaneously. The power of the reference beam is 7µW and that of the signal beam is about 300nW. The relaxation time or the time

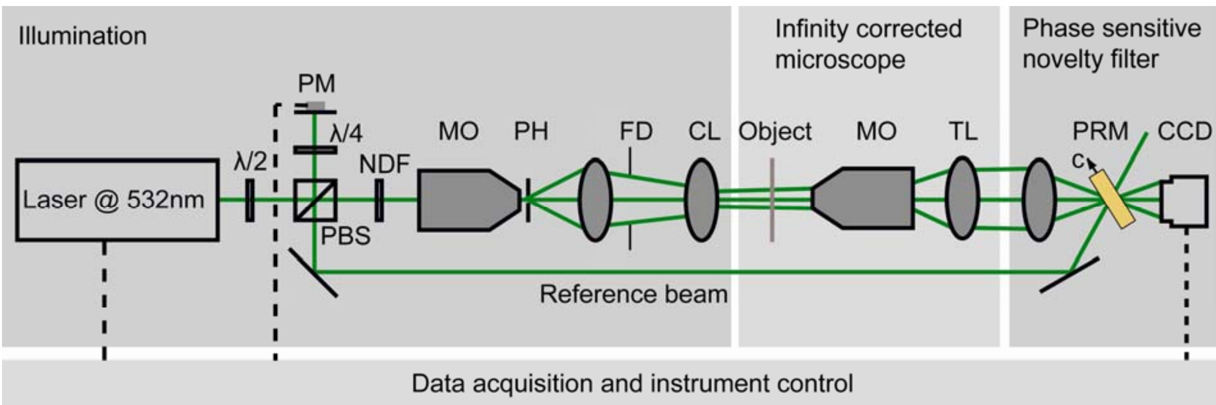


Fig.4 - Sketch of a novelty filter microscope setup. The setup can be devided into three main parts: illumination, infinity corrected microscope and novelty filter. PM: piezo mirror, λ/2: half-wave plate, λ/4: quarter wave plate, PBS: polarizing beam splitter, NDF: neutral density filter, MO: microscope objective, PH: pinhole, FD: field diaphragm, CL: condenser lens, TL: tube lens, c: optical axis, PRM: photorefractive BaTiO3 crystal, CCD: camera

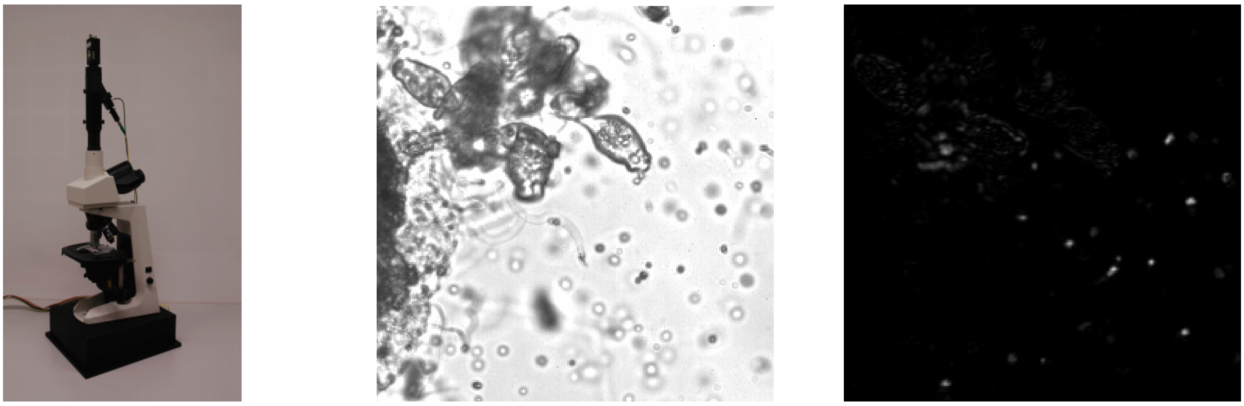

Fig. 5 – Novelty filtering. a) Left: application NFM. b) Middle: original image. c) Right: the same image scene after optical novelty filtering with the NFM.

constant for the grating build-up in the crystal is about 20s. The choice of this large time constant helps to suppress trail formation and thus allows one-to-one imaging of moving objects in real-time [14].

Fig. 5 (to the left) shows a photograph of a novelty filter, implemented in a commercial infinity corrected microscope. This modularized system has been filed for a patent at the German Patent and Trade Mark Office. Fig. 5 (in the middle and to the right) gives an impression of the effect the ONF has on image sequences. The illustration in the middle shows a snapshot of the fluid flow, the illustration to the right depicts the result of ONF applied to the image sequence. Obviously, all static background information like the biofilm on which the ciliate grows or the stationary ciliates zooid is suppressed by the ONF. The more novelty a pixel represents, the brighter it appears in the ONF filtered image. Thus in the presented scene it can e. g. be concluded, that the ciliates (light grey shade) move slowly, where the bright spots give the positions of moving particles.

## 2.2 GPU reconstruction

### *2.2.1 Model Based Reconstruction of Flow Fields from Experimental Particle Sequences*

The reconstruction method used in this paper is inspired by the non-parametric image registration technique currently used in medical imaging. It is a common task in medicine to find the correspondence between the images of the same anatomical structure taken under the different conditions (e.g. different relative camera-patient position, different methods of acquisition, etc.). More precisely, given two images - *reference* image $R$ and *template* image $T$ – the task is to find a transformation, which deforms $T$ in such a way, that the difference between $T$ and $R$ is minimal. Since, the non-parametric minimization problem is ill-posed at the origin, it is usually solved using the regularization term, or *smoother* $S$, which can be chosen based on the laws of physics. For example, the so called *fluid registration* suggests to build $S$ upon the Navier-Stokes equations.

All the motion estimation techniques for reconstruction of velocity fields from the PIV-sequences can be roughly classified as based on optical flow (OF) computation [10] and cross-correlation analysis [11]. Most of these standard techniques calculate the vector field without taking the properties of the underlying flow into consideration. In this way, the resulting vector fields often contain physically irrelevant structures.

In contrast, the reconstruction method used in this paper integrates a priori knowledge about the induced flow into the analysis. Thus, generated vector fields are consistent with the underlying flow model. However, the model suitable for efficient coupling with the evaluation process must be found.

*Method description*. The image registration solves the problem similar to the extraction of vector fields from the experimental particle image sequences. Thus, the reconstruction method for PIV-sequences can be build upon the *predictor-corrector* scheme, widely used in image registration. However, some global modification of the generic scheme should be done:

1. Compute (*predict*) the vector field by means of standard OF,
2. *Correct* the output of the OF computation using the solution of Navier-Stokes equations,
3. Repeat prediction and correction iteratively over the *deformed* template and original reference images
4. Implement all the steps of the algorithm on programmable graphics card (GPU) in order to make the process of reconstruction *and* visualization interactive.

The summary of the algorithm is presented in Fig. 6.

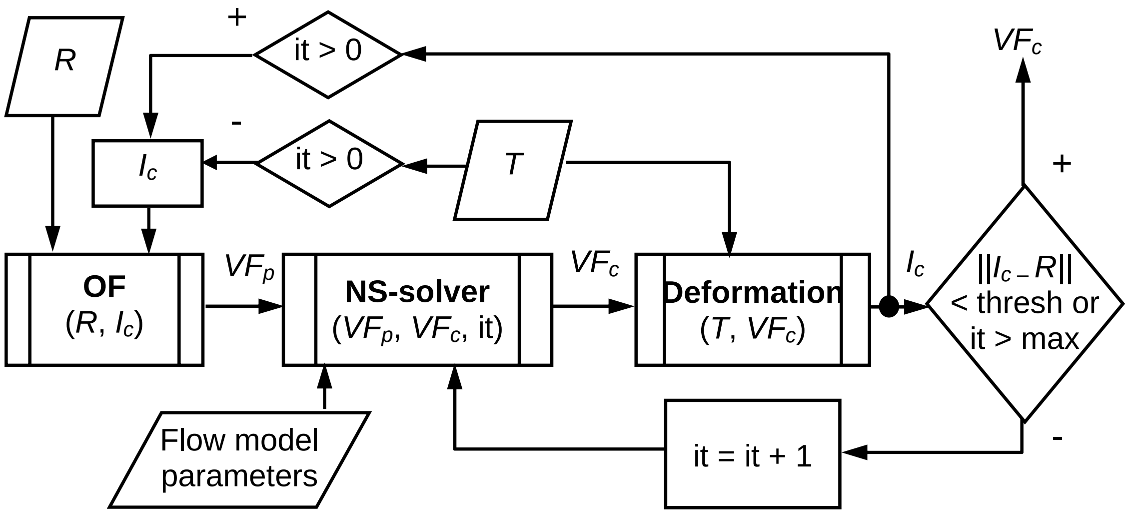


Fig. 6 - Overview of predictor-corrector method for reconstruction of vector field from PIV-images

The main idea of our algorithm is to *deform* iteratively $T$ in such a way, that the difference between $T$ and $R$ will be minimized. During this process the image deformations are accumulated and the resulting deformation is considered as the reconstructed displacement field. In each iteration the displacement field ($VF_p$) is *predicted* using the classical OF method. On the next step $VF_p$ is *corrected* into $VF_c$ using the solution to the incompressible Navier-Stokes equations. The correction step is followed by the *deformation* of $T$ along the corrected displacement field $VF_c$. At the end of the cycle the deformed image $I_c$ is compared to $R$. If the difference between the images is smaller than the user specified threshold, the process stops and the currently computed $VF_c$ is returned.

*Vector field correction*. In order to correct the vector field estimated by the OF, the numerical solution of unsteady incompressible Navier-Stokes equations with $U$ the velocity vector, $P$ the pressure and the external force vector $F$ is used:

$$\frac{\partial U}{\partial t} = \frac{1}{\mathrm{Re}}\Delta U - (U \cdot grad)U - grad\, P + F, \quad divU = 0. \qquad (2)$$

On the very first iteration of the proposed algorithm the OF solution is used as a guess for the initial velocity field in Navier-Stokes simulation. Moreover, if experiment settings include an obstacle, the additional boundary conditions at the border of this obstacle are extracted from the images and taken into account. The following solution of the Navier-Stokes equation corrects the predicted vector field and generates the result which is suited to be physically correct. However, after the first iteration it could happen that the computed vector field still significantly deviates from the actual one. Consecutive iterations serve to treat this problem.

In order to move to the next iteration, the template image $T$ is deformed "back" towards the reference image $R$. On the following iteration the OF displacement field $VF_c$ is computed between $R$ and $I_c$. Via deformation the difference between $R$ and $I_c$ progressively decreases. In contrast to the first iteration, the velocity field on the further iterations is inserted as external force field into the Navier-Stokes simulation. The whole process is repeated until the average force amplitude become less than the user specified threshold or the maximum number of iterations is achieved.

*Image deformation.* Once the displacement field (in pixels) is computed *and* corrected by the Navier-Stokes solver, we *deform* the template image $T$ in texture coordinate space towards the reference image $R$. This operation is performed efficiently on the GPU: displacement values are simply read from the corresponding texture, converted into texture coordinate space (scaled to fit into the range [0;1]) and then used to fetch the values of template image. If some pixels are addressed beyond the valid image area, the corresponding image border pixels are repeated instead. From Fig. 7 one can see that vector field reconstructed by our algorithm is significantly different than the vector field computed by pure OF. There is only one parameter to be changed in OF

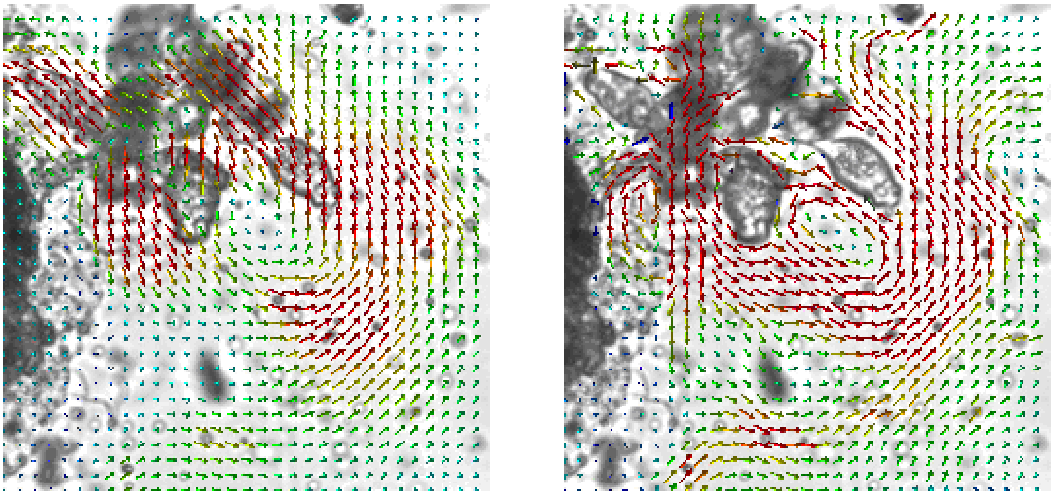

Fig. 7 – Vector field reconstructed using: a) (to the left) pure OF with high weight of regularization term, b) (to the right) proposed model-based algorithm

solution: the weight of regularization term. Obviously, this is not enough: if a high weight of regularization term leads to smearing out of important flow features, a small weight causes extraction of non-existing features and violation of flow continuity. On the other hand, after each iteration of the proposed model-based algorithm, those features become more distinguishable and satisfy the underlying flow model.

## 4 CONCLUSIONS AND OUTLOOK

This paper presents a novel neuronumerical hybrid for the detection of reconstruction artefacts. It is based on the implementation of numerically expressed a priory knowledge on the flow field (Taylor-hypothesis) into an artificial neural network as a functional node. The proper functionality of the neurohybrid is demonstrated at an example from microfluidics i. e. the microorganismic generated flow patterns induced by sessile ciliates. The neuronumerical hybrid has been proven to detect reliably spurious velocity vectors. Additionally, it provides a suitable means for further exploration of such phenomena like the contraction of the zooid as shown in the example.

The neurohybrid is basically applied on images generated by an inverse microscope, but it can also be combined with non-linear optical novelty filtering (ONF), which offers additionally advantages due to the enhancement in contrast and the removing of quiescent objects. To be more precise, due to the ONF working as a temporal high pass filter all time-independent information such as the background is blocked instantaneously. Furthermore, and for the case of the microorganismic induced flow of great advantage, the use of the ONF allows an extended observation time while strictly keeping the necessary biocompatibility. Concerning the evaluation of the image data, the model-based reconstruction method on the GPU presented in this paper allows for the interactive and physically correct reconstruction of vector fields from sequences of particle images. The main advantages of this reconstruction method are the coupling of a high resolution motion estimation technique with the underlying physical model and interactivity. The first results demonstrate improved quality of reconstructed vector fields. Particularly, the structures extracted by the standard image processing algorithm but being inconsistent with the underlying flow model are automatically removed. Moreover, efficient implementation of the method on the GPU allows for interactive selection and change of model-specific parameters.

## REFERENCES


1. Hartmann, C., Özmutlu, Ö., Petermeier, H., Fried, J., Delgado A., Journal of Biomechanics, 2006 (In press)
2. Krishnamachari, V.V., Denz, C., J. Opt. A: Pure Appl. Opt. 5, 239 (2003)
3. Krüger, J., Schiwietz T., Kipfer, P., Westermann, R., Proceedings ParSim (2004)
4. Anderson, D.Z. and Feinberg, J., IEEE J. Quantum Electron., Vol. 25, 635 (1989)
5. Anderson, D.Z., Lininger, D.M. and Feinberg, J., Optics Letters, Vol. 12, 123 (1987)
6. Sedlatschek, M., Trumpfheller, J., Hartmann, J., Müller, M., Denz, C., and Tschudi, T., Appl. Phys. B: Lasers Opt. 68 1047 (1999)
7. Krishnamachari, V. V. , Denz, C., J. Opt. A, Pure Appl. Opt. 5, 239 (2003)
8. Krishnamachari, V. V., Denz, C., Appl. Phys. B: Lasers Opt. 79, 497 (2004).
9. Krishnamachari, V.V., Grothe, O., Deitmar, H., Denz,C., Appl. Phys. Lett. 87 071105 (2005)
10. Horn, B. K. P., Schmuck, B. G., Artificial Intelligence, 17, 185 (1981)
11. Raffel, M., Willert, C., Kompenhans, J., Springer-Verlag, Heidelberg (1998)
12. Fellner, M., Delgado, A., Becker, T., Bioprocess and Biosystems Engineering 25, 263 (2003)
13. Petermeier, H., Baars, A., Delgado, A., Proceedings 13. GALA 2005, S. 12.55-1-12.55-6, Cottbus 6.-8.9.2005
14. Taylor, G. I., Proc. Roy. Soc. London A, vol. 164, 476, (1938)